jove

In Vivo Wide-Field and Two-Photon Calcium Imaging from a Mouse using a Large Cranial Window

Satoshi Manita[1], **Eiji Shigetomi**[2,3], **Haruhiko Bito**[4], **Schuichi Koizumi**[2,3], **Kazuo Kitamura**[1]

[1] Department of Neurophysiology, Faculty of Medicine, University of Yamanashi [2] Department of Neuropharmacology, Faculty of Medicine, University of Yamanashi [3] Yamanashi GLIA center, Interdisciplinary Graduate School of Medicine, University of Yamanashi [4] Department of Neurochemistry, Graduate School of Medicine, The University of Tokyo

Corresponding Authors

Satoshi Manita
smanita@yamanashi.ac.jp

Kazuo Kitamura
kitamurak@yamanashi.ac.jp

Citation

Manita, S., Shigetomi, E., Bito, H., Koizumi, S., Kitamura, K. *In Vivo* Wide-Field and Two-Photon Calcium Imaging from a Mouse using a Large Cranial Window. *J. Vis. Exp.* (186), e64224, doi:10.3791/64224 (2022).

Date Published

August 4, 2022

DOI

10.3791/64224

URL

jove.com/video/64224

Abstract

Wide-field calcium imaging from the mouse's neocortex allows one to observe cortex-wide neural activity related to various brain functions. On the other hand, two-photon imaging can resolve the activity of local neural circuits at the single-cell level. It is critical to make a large cranial window to perform multiple-scale analysis using both imaging techniques in the same mouse. To achieve this, one must remove a large section of the skull and cover the exposed cortical surface with transparent materials. Previously, glass skulls and polymer-based cranial windows have been developed for this purpose, but these materials are not easily fabricated. The present protocol describes a simple method for making a large cranial window consisting of commercially available polyvinylidene chloride (PVDC) wrapping film, a transparent silicone plug, and a cover glass. For imaging the dorsal surface of an entire hemisphere, the window size was approximately 6 x 3 mm^2. Severe brain vibrations were not observed regardless of such a large window. Importantly, the condition of the brain surface did not deteriorate for more than one month. Wide-field imaging of a mouse expressing a genetically-encoded calcium indicator (GECI), GCaMP6f, specifically in astrocytes, revealed synchronized responses in a few millimeters. Two-photon imaging of the same mouse showed prominent calcium responses in individual astrocytes over several seconds. Furthermore, a thin layer of an adeno-associated virus was applied to the PVDC film and successfully expressed GECI in cortical neurons over the cranial window. This technique is reliable and cost-effective for making a large cranial window and facilitates the investigation of the neural and glial dynamics and their interactions during behavior at the macroscopic and microscopic levels.

Introduction

Wide-field calcium imaging effectively investigates the spatiotemporal activity pattern over a large area of the animal brain[1,2,3]. Wide-field imaging has been extensively used to observe rodents' entire cortical surface since their cortex is relatively flat[2,3,4,5,6,7,8,9,10]. Transgenic mice or mice injected with adeno-associated virus (AAV), which specifically express GECIs in various cells such as neurons and glial cells, can be used for wide-field calcium imaging[11,12,13]. However, the spatial resolution of this technique is usually not enough to resolve the activity of individual cells *in vivo*[14]. It is also not suitable for imaging cells located in deeper layers.

On the other hand, two-photon calcium imaging can observe the activity of multiple cells simultaneously with subcellular spatial resolution, allowing the observation of the activity of individual cells even in neuronal dendrites and glial processes[15,16,17,18,19,20,21,22]. It can also observe cells in deeper layers of the cerebral cortex[23,24]. Although recent technological advances in two-photon microscopy enable imaging from millimeter-wide cortical regions[25,26,27,28,29], it is still difficult to observe an area comparable to wide-field imaging by two-photon imaging.

To understand the physiological relevance of brain activity from single-cell to whole-brain, it is critical to bridge the gap between the activity of cortical regions over the entire cortex and that at single-cell resolution in local neural circuits. Therefore, a combination of wide-field and two-photon calcium imaging performed in the same mouse is especially effective. To realize this, a wide and stable cranial window must be created, ideally over a long period.

Previously, several techniques for making cranial windows have been developed to allow wide-field and two-photon imaging to be performed in the same mouse[30,31]. Trapezoidal-shaped cover glass windows (crystal skull), which are molded into the shape of the cortical surface to replace the removed bone, allow optical access over the entire cortex[32]. Alternatively, polymer-based cranial windows can be made with polyethylene terephthalate (PET)[33] or polyethylene-oxide-coated amorphous fluoropolymers nanosheet[34]. Each method has been shown to maintain a stable window for more than 1 month. However, producing these windows is not easy, and the materials and equipment used are often expensive.

The present study describes a new method for making a large cranial window using the PVDC film (plastic food wrap) (**Figure 1**). Using this window, *in vivo* wide-field and two-photon imaging experiments can be performed in the same mice. It has also been shown that GECIs could be expressed in neurons over a wide area of the cortex of mice by forming a thin layer of film containing AAV particles on the wrap.

Protocol

The experimental procedures were approved by the Animal Experiment Committee of University of Yamanashi. Wild-type (C57BL/6J, Japan SLC) and transgenic mice expressing membrane-anchored GECI (Lck-GCaMP6f) in astrocytes were used in this study. The transgenic mice were obtained by crossing AldH1l1-CreERT2 mice [B6N.FVB-Tg(Aldh1l1-cre/ERT2)1Khakh/J, commercially obtained, see **Table of Materials**] and Flx-Lck-GCaMP6f mice [C57BL/6N-Gt(ROSA)26Sor<tm1(CAG-GCaMP6f)Khak>/J, commercially obtained] mice. The transgenic mice were treated with tamoxifen (20 mg/mL) for 5 days (0.05 mL/10 g bw, i.p.) to express GCaMP6f. All mice

used were males and females at least 4 weeks old. The schematic of the window is shown in **Figure 1A**, and the surgical procedure is summarized in **Figure 1B**.

1. Preparation for cranial window surgery

1. Anesthetize mice with isoflurane (induction: 3%, surgery: 1%-1.5%, flow rate: 0.2-0.3 L/min). Confirm the depth of anesthesia by the loss of tail or toe pinch reflex. Maintain the body temperature using a heating pad (36-38 °C). Apply eye ointment with a cotton swab to prevent the eyes of mice from drying out under anesthesia.
2. Inject 15% mannitol solution (see **Table of Materials**) intraperitoneally (3 mL/100 g body weight). Fix the head of the mouse on a stereotaxic frame with ear bars. Remove hair from the head of the mouse using a shaver and hair removal cream.
3. Disinfect the skin surface with povidone-iodine and alcohol three times**.** Apply Lidocaine topically to provide preemptive analgesia. Remove the skin over the area of interest with surgical scissors and expose the skull (size: 15 x 15 mm). If bleeding is present, use a cotton swab to stop the bleeding.
   NOTE: In this study, the skin was removed to observe the prefrontal cortex to the visual cortex.
4. Remove the periosteum over the exposed skull using a micro curette and dry the skull surface to firmly attach the head plate to the skull with dental cement (see **Table of Materials**) (**Figure 2B**).
   NOTE: The custom-made head plate is created using a 3D printer. The design file is deposited to the Github repository (https://github.com/Satoshi-Manita/Head-plates).
5. Attach the head plate using dental cement (**Figure 2C**). Wait at least 20 min for the cement to harden. Secure the head plate with the head plate holder[35].

2. Making the cranial window

1. Remove the extra cement over the skull with a dental drill (see **Table of Materials**). Be careful not to drill through the bone and damage the brain by drilling.
2. Mark the area to be cut with a pen and cut into the bone with a scalpel. Blunt the tip of the scalpel to ensure that the tip does not penetrate the skull (**Supplementary Figure 1**). Reference the brain atlas to determine where to make the window.
   NOTE: For the present study, a window was created between -2 mm and +4 mm from bregma in the anteroposterior axis and from sagittal suture to +3 mm in the mediolateral axis, including the motor, somatosensory, and visual cortices.
3. Scrape the bone repeatedly with a scalpel to deepen the groove until the bone in the area to be trimmed moves well when lightly touched.
4. Remove the incised bone with fine tweezers. Do not push the bone flap into the brain, which may damage the brain (**Figure 1B$_a$**).
   NOTE: If bleeding is observed after removing the bone, immediately apply and aspirate artificial cerebrospinal fluid (ACSF, see **Table of Materials**) and repeat this process until the bleeding stops. Alternatively, place a hemostatic gelatin sponge (about 3 mm square cubes) soaked in the ACSF on the bleeding point.
5. If the dura is not removed, proceed to step 2.7.
6. Remove the dura mater following the steps below.

1. Remove the dura, for example, in the following situations; transfection using the fibroin-AAV film method[36] and observing small structures such as dendritic spines.
2. Cut the dura using a pulled glass pipette with a tapered tip of about 10 µm. To expand this cut over the entire window, use a U-shaped needle.
3. Set the stereomicroscope zoom to 60-100x and remove the severed dura mater with ultrafine tweezers. If removing the dura mater causes bleeding, rinse with ACSF or use a gelatin sponge to stop the bleeding.

7. Cut out the PVDC wrap.
   1. Sterilize a large (for example, 10 x 15 mm) piece of PVDC wrap (about 11 µm, see **Table of Materials**, **Figure 2A$_a$**) by autoclaving and with 70% ethanol.
   2. Under a stereomicroscope, use tweezers and a scalpel to cut out a wrap of the required size.
      NOTE: The wrap size needs to be approximately 10 mm larger than the size of the cranial window but smaller than the opening of the head plate. For a 6 x 3 mm^2 cranial window, prepare a 15 x 10 mm^2 wrap.
8. Place the wrap accurately following the steps below.
   1. Place the wrap on the brain surface, leaving the ACSF on the surface. Suck out the ACSF from the edge of the wrap, allowing the wrap to stick firmly to the brain surface (**Figure 1B$_{b,c}$**).
      NOTE: The wrap used is wrinkle-resistant, so just placing it on the brain's surface produces almost no wrinkles.
   2. Trim the wrap with a scalpel and tweezers so that there is approximately a 1 mm margin between the edge of the cranial window and the wrap (**Figure 1B$_d$**).
   3. Once the wrap is in place, glue the edge of the wrap to the skull with a biological adhesive (see **Table of Materials**, **Figure 2D**). Allow the adhesive to dry for about 30 min.
9. Apply the transparent silicone elastomer.
   1. Apply the commercially available transparent silicone elastomer (see **Table of Materials**) on top of the wrap using a dispenser with a mixing tip (**Figure 1B$_e$, 2A$_{b-d}$**) and place the cover glass (0.12-0.17 mm thickness) on top (**Figure 2E**).
   2. Seal the perimeter of the cover glass with waterproof film, superglue, or dental cement (**Figure 1B$_f$**).
10. After surgery, monitor the mouse until it regains consciousness to maintain sternal recumbency. After that, keep the mice individually, and allow them to recover in their home cage for at least 7 days.
    1. To reduce stress and pain, administer anti-inflammatory and analgesic agents (e.g., dexamethasone and ketoprofen, 5 mg/kg each, i.p.).
11. Monitor the mice regularly for infection. If an infection is confirmed, administer an antimicrobial drug (e.g., 10 % enrofloxacin, 1.7 µL/mL) in the drinking water until the infection is eliminated (typically less than 4 weeks).

3. Making AAV film on plastic wrap using fibroin solution

NOTE: Step 3 is optional.

1. Prepare fibroin solution from silkworm cocoons following a previously published method[37].

1. In brief, boil commercially available normal silkworm cocoons (5 g, see **Table of Materials**) in sodium carbonate solution (0.02 M, 2 L). Wash the cocoons in ultrapure water and dry overnight.
2. Dissolve the dried cocoons in lithium bromide solution (9.3 M, 20% w/v fibroin) while heating in an oven at 60 °C for 4 h. Dialyze the dissolved cocoon solution, centrifuge (twice at 12,700 x *g*, at 4 °C for 20 min)[37], and collect the supernatant.

2. Prepare the fibroin-AAV film following the steps below.
   1. Mix fibroin and AAV solutions[20] in a 1:4 ratio in a small sample tube using a micropipette. Drop an aliquot of the mixed fibroin-AAV solution onto the plastic wrap for the cranial window, and dry it for at least 3 h.
      NOTE: For expression in an area of 3 mm in diameter, apply a 5 µL drop of fibroin-AAV solution. This ratio determines the amount of solution for a given area.
   2. After drying, cut the plastic wrap into the required size for the window (for example, 10 x 15 mm) and place it on the brain surface. Then, follow the abovementioned method from step 2.8.1 onward.
      NOTE: Before placing the wrap on the brain surface, remove the ACSF on the brain surface as much as possible. This is because the ACSF is expected to dissolve the fibroin-AAV film and reduce the concentration of AAV particles.
   3. Wait about 2-4 weeks after creating the AAV-treated window until the GECIs are expressed sufficiently. During this process, check the condition of the mice and windows regularly.

4. Calcium imaging and analysis

NOTE: For details on the imaging and analysis, please see previously published reports[1,2,38].

1. Perform wide-field imaging following the steps below.
   1. Immobilize the mouse using a head fixation device under a tandem lens fluorescence macroscope (see **Table of Materials**).
   2. Illuminate the cerebral cortex of mice with excitation light from a 465 nm LED light source through an excitation filter, dichroic mirror, and objective lens.
   3. Collect the fluorescence images of the cerebral cortex by a CCD camera through an objective lens (1.0x), dichroic mirror, emission filter, and imaging lens (2.0x). The combination of these lenses gives a total magnification of about 0.5x.
   4. Acquire images at a sampling frequency of 50 Hz. After data acquisition, analyze the images using ImageJ software. Select the region of interest (ROI) manually. Calculate fluorescence change in each ROI as ΔF/F = (Ft - F0) / F0, where Ft is the raw fluorescence value of each frame and F0 is the mean fluorescence value obtained from an average image of all frames.
      NOTE: A macro program for ImageJ is deposited to GitHub (https://github.com/Satoshi-Manita/ImageJ-macro), which calculates ΔF/F images from calcium imaging data.
2. Perform two-photon imaging following the steps below.
   1. Immobilize the mouse under a two-photon microscope using a head fixation device. Identify the area to be imaged using the microscope in bright-

field mode with a low magnification (5x) objective lens.

2. Switch to two-photon imaging. Use a high magnification objective lens (16x or 25x) and illuminate the laser for two-photon excitation.

   NOTE: Green Lck-GCaMP6f[22] and red XCaMP-R[36] were excited by an ultrafast laser at excitation wavelengths of 920 nm and 1070 nm, respectively.

3. Acquire fluorescence images at 30 Hz. After data acquisition, correct motion artifacts by the registration function of the suite2p software[39]. Obtain ROI and ΔF/F from images using the same method for wide-field imaging.

3. Plot the data using python with the following libraries: NumPy, Matplotlib, and Pandas (see **Table of Materials**).

Representative Results

Evaluation of a large cranial window made using the PVDC wrap methods

Immediately after the surgery, success or failure can be checked at a glance by the condition of the cortical surface, such as bleeding and color change due to damage or ischemia. A long time after surgery, the cortical surface may be covered with an opaque white membrane due to infection, or blood may cover the window due to bleeding (**Figure 2G**). In these cases, the cortex may not be in healthy condition, and imaging may not be possible. These could be caused by partially severed wraps or insufficient fixation of the wrap by the adhesive. If the infection is repeatedly observed, it may be effective to apply antibiotics, for example, gentamicin sulfate (10 µL, 50 mg/mL), over the brain surface at window placement. Regeneration of meninges or bones is also seen when the vertical gap between the cortical surface and the wrap is large. To prevent this, applying the wrap as tightly as possible to the brain surface during window preparation is crucial. This can be achieved by placing plastic wrap on the brain surface and sucking out as much ACSF as possible. In the absence of ACSF, it can be done by simply placing the plastic wrap on the brain surface. The brain and blood vessels are determined to be undamaged by the fact that the color of the brain is not discolored and blood vessels are not severed.

The longevity of the window largely depends on the quality of the surgery. When the condition is good, there is no sign of infection, bleeding, or regeneration more than 1 month after surgery (**Figure 2F** and **Figure 3B**). In 8 of 10 mice, the window could be maintained clear up to 10 weeks or longer. Windows in two of the mice could not be properly maintained due to infection or bleeding. Although the large window may be prone to mechanical stress or impact, broken or cracked windows were not observed.

To evaluate the imaging quality of the new cranial window with the wrap, silicone, and glass, the point spread function was compared under the new window with that under the conventional glass window by imaging 0.1 µm fluorescent beads in agar (see **Supplementary File 1**). The results showed no difference in full width at half maximum (FWHM) for both conditions. [X-axis (µm): glass only, 1.99 ± 0.07, wrap, 1.76 ± 0.13, Y-axis (µm): glass only, 2.11 ± 0.27, wrap, 1.90 ± 0.15, Z-axis (µm): glass only, 25.29 ± 0.71, wrap, 26.64 ± 1.02, N = 7 beads, $p > 0.05$, the Mann-Whitney U test, **Supplementary Figure 2A,B**]. Therefore, the new elements added (wrap and silicone) did not deteriorate the imaging quality.

Vibration artifacts caused by respiration, heartbeat, and body movement are present in wide-field and two-photon imaging.

To determine how much the new cranial window vibrates, a small fluorescent particle was selected from the *in vivo* two-photon imaging data and examined how much its image moved during 60 s. It was found that the standard deviation of the centroid of that fluorescent particle was about 0.3 µm, which is comparable to that under a conventional glass window (**Supplementary Figure 2C**). This indicates that because the brain was held down by a transparent silicone plug and cover glass, the vibrations were comparable to that observed in conventional smaller windows, and offline image registration was sufficient to eliminate vibration artifacts.

In wide-field calcium imaging, the cortical activity could be observed propagating across the cortex induced by sensory stimulation (**Figure 3A-D,K-N**). Two-photon imaging allowed the observation of single-cell fluorescence images specific to neurons and glial cells (**Figure 3E,O**). Fluorescence changes induced by sensory stimulation could be observed in individual cells (**Figure 3E-J,O-T**).

Expression of genetically-encoded calcium indicators (GECIs) in a wide area of the cerebral cortex using the PVDC wrap and AAV

The PVDC wrap for the window could be applied to express functional proteins in a wide area of the cortex. This is achieved using AAV and fibroin, a component protein of silkworm cocoons that have been widely applied as biomaterials[37]. A previous study showed that fibroin could be mixed with AAVs, forming films implanted in the brain to express functional proteins such as photoactivable opsins or GECIs[36]. In the present study, AAV expressing GECI and fibroin were mixed and dried on the wrap, and AAV-coated wrap was used for the cranial window. This resulted in the expression of GECI over the broad area of the cortex 2-4 weeks after surgery (**Figure 3K-M**). Since the window was large, different cortical areas of the same mouse can be imaged (**Figure 3M-T**).

To confirm the expression efficiency of this method, the number of cells expressing GECI was counted in the fixed brain (**Supplementary Figure 2D**). It was found that the present strategy using the wrap with fibroin-AAV resulted in the expression of GECI with an efficiency of approximately 20% in both superficial and deeper layers (L2/3: 20.78%, XCaMP-R expressing cell: 32 cells, DAPI: 154 locations, L5: 20.08%, XCaMP-R expressing cell: 51 cells, DAPI: 254 locations). Thus, this method expressed GECIs in cells not only in surface layers but also in deeper layers.

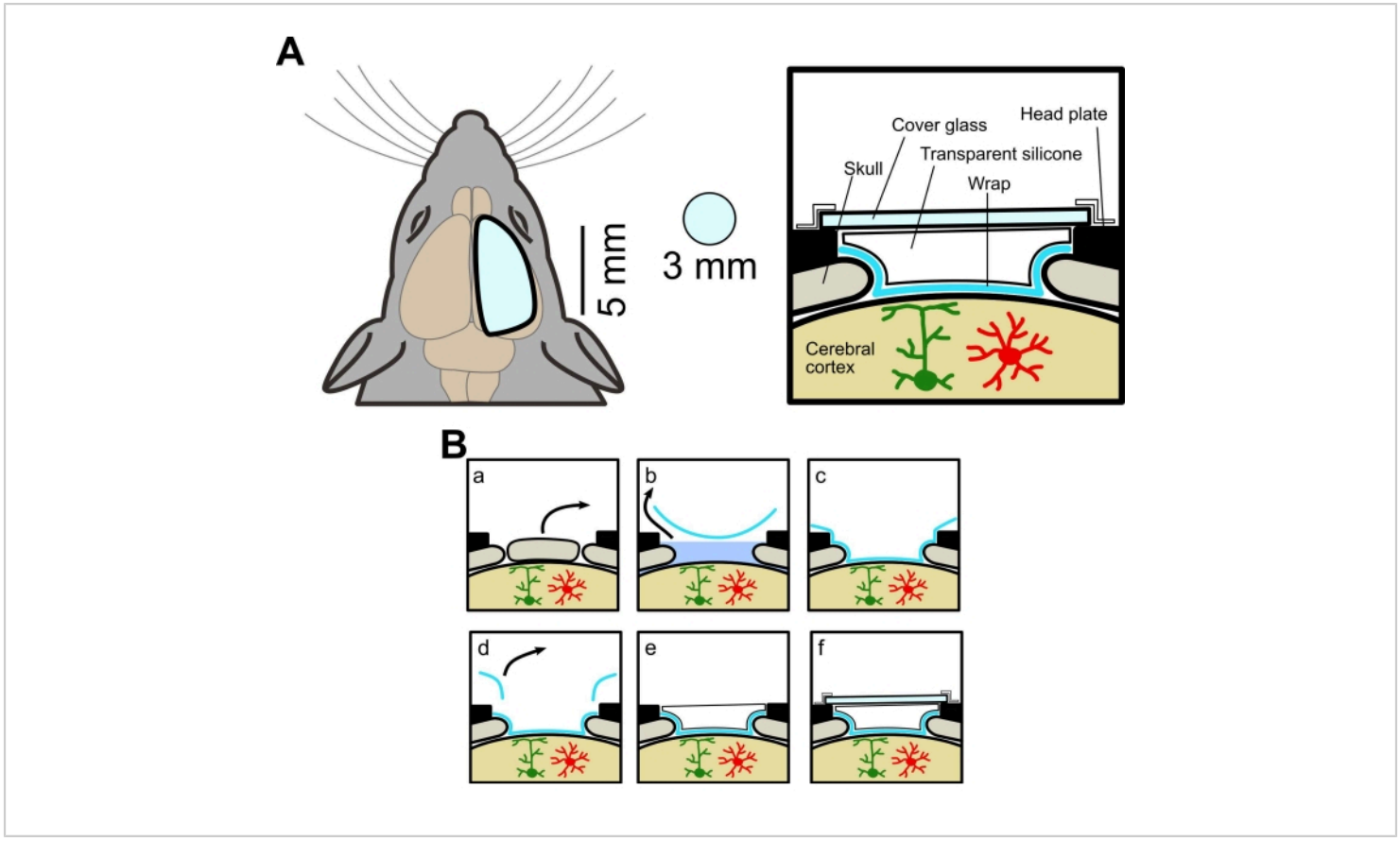

Figure 1: Conceptual diagram of the large cranial window. (**A**) Left, schematic drawing of the new cranial window. It is larger than the conventional window (3 mm diameter). Right, Cross-sectional view. The method for making a large cranial window uses food wrap, transparent silicone elastomer, and cover glass, allowing wide-field and two-photon imaging from the same mouse. (**B**) Cranial window fabrication procedure: (**a**) Bone removal. (**b**) Removal of ACSF under the wrap. (**c**) Adherence of the wrap to the brain surface by removing ACSF. (**d**) Cutting away the excess wrap. (**e**) Applying transparent silicone. (**f**) Affixing cover glass. Please click here to view a larger version of this figure.

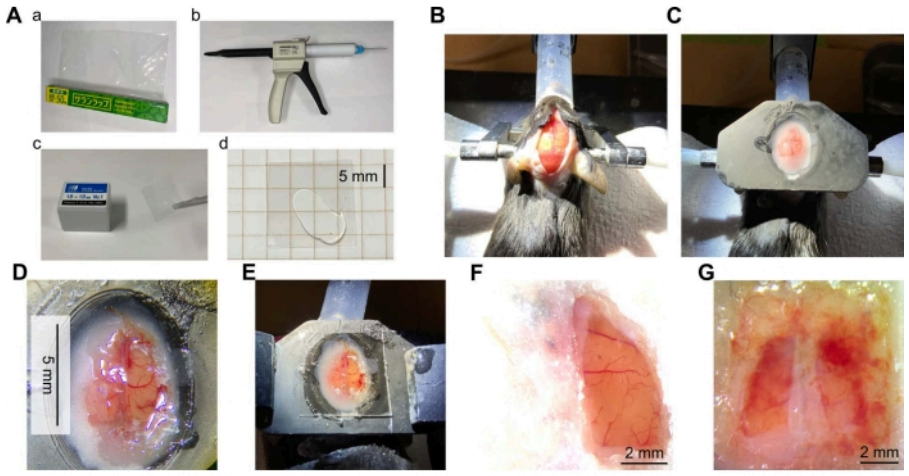

Figure 2: Overview of cranial window surgery. (**A**) Materials and equipment required for the cranial window. (**a**) Polyvinylidene chloride (PVDC) wrapping film. (**b**) A dispenser of transparent silicone elastomer with a mixing tip. (**c**) Cover glass. (**d**) Transparent silicone placed between two pieces of the cover glass. (**B**) Photograph of mouse head skin incised to expose the skull. The mouse was anesthetized, and the head of the mouse was immobilized using ear bars. The head was then dehaired, treated with local analgesia, and the skin was incised. (**C**) Photograph after installation of a head plate. A head plate (made of resin from a 3D printer) was attached to the head of the mouse with dental cement. (**D**) Photograph of a cranial window. The cranial window was created in the cortex of the right hemisphere of the mouse brain. The dura mater was removed, and the wrap was glued in place. (**E**) A photo of the window made of the wrap with the transparent silicone and cover glass on top. (**F**) A typical example of a successful window (right hemisphere, 7 weeks after surgery). (**G**) Example of failed window (both hemispheres, 5 weeks after surgery). Please click here to view a larger version of this figure.

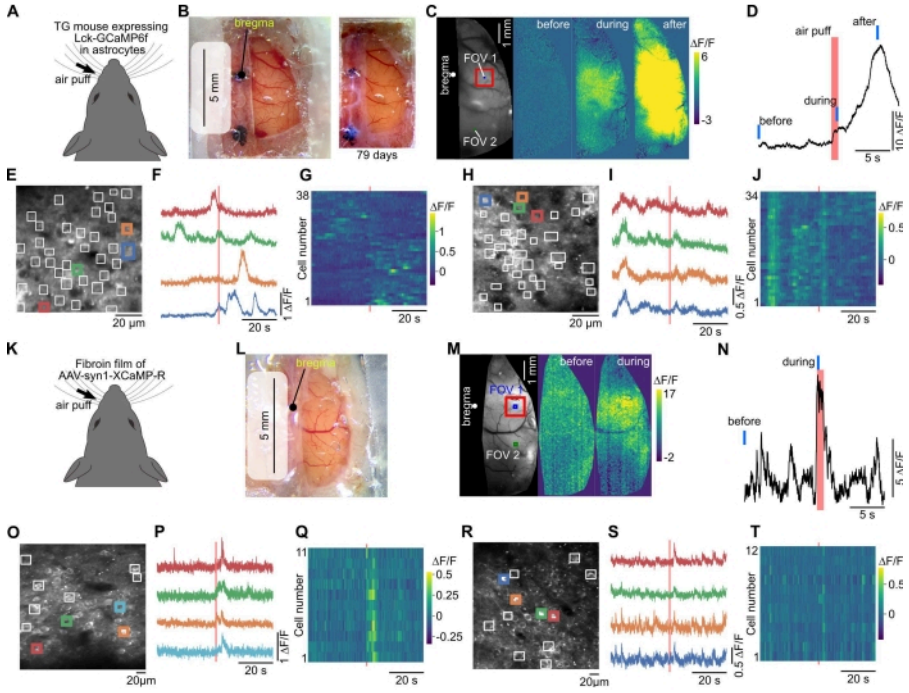

Figure 3: The large window allows wide-field and two-photon calcium imaging from the same mouse. (**A**) Calcium imaging was performed in a transgenic mouse expressing membrane-anchored GECI (Lck-GCaMP6f) in astrocytes[40]. (**B**) Left, a large window was created with plastic wrap, transparent silicone, and cover glass. Wide-field imaging was performed through this window. Right, a photo was captured 79 days after the installation of the cranial window. (**C**) When air-puff stimulation was applied to the contralateral whiskers, fluorescence changes were observed. (**D**) The time course of the fluorescence change in the somatosensory cortex (red square in **C**) was plotted. Red and blue bars indicate air puff timing and "before", "during", and "after" timing in (**C**), respectively. (**E**) The field of view (FOV 1 in **C**) of two-photon calcium imaging. Because GCaMP6f was expressed to localize to the membrane, the regions of interest (white squares) were manually placed to detect the local response in astrocyte processes. (**F**) The fluorescence changes in the colored squares in (**E**) are plotted. (**G**) The fluorescence changes in all squares of (**E**) are plotted. Horizontal and vertical axes indicate time and cell number, respectively. (**H-J)** Data for FOV 2 (in the visual cortex) in (**C**) are shown. The FOV 2 was imaged after the imaging in the FOV 1. (**K**) Red GECI, XCaMP-R, was expressed in neurons by the fibroin-AAV method in the wild-type mouse. (**L**) Photograph captured two weeks after surgery in which the window was created using the fibroin film. (**M**) Wide-field calcium imaging was performed on this mouse. (**N**) The fluorescence change evoked by whisker stimulation was plotted from the most prominent site (somatosensory cortex, red square in (**M**)). Red and blue lines indicate air puff timing and "before" and "during" timing in (**M**), respectively. (**O**) Field of view (somatosensory cortex, FOV 1 in (**M**)) of two-photon calcium imaging at 300 μm depth. ROIs were manually placed at neuronal somata. (**P**) The fluorescence changes in the

colored squares in (**O**) are plotted. (**Q**) The fluorescence changes in all squares of (**O**) are plotted in color. (**R-T**) Data for FOV 2 in (**M**) located in the parietal cortex are shown. Please click here to view a larger version of this figure.

Supplementary Figure 1: Tips for scalpels. The tip of the new scalpel (top) compared to the scalpel used to cut the skull with a blunted tip (bottom). Please click here to download this File.

Supplementary Figure 2: Validation of the new cranial window and the fibroin-AAV expression method. (**A**) Fluorescence intensity profile of the 0.1 µm fluorescent beads in agar. The top row shows data from a condition in which only cover glass was placed over fluorescent beads mixed in agar, and the bottom row shows data from a condition in which wrap, transparent silicone, and cover glass were placed. The gray traces show the Gaussian fit to the fluorescence intensity profile for each bead, and the red traces show their average values (n = 7). (**B**) Summary of data in (**A**). Each graph shows the full width at half maximum (FWHM) of the point spread function on the XYZ axis. The gray plot shows the data for each bead, and the red shows their mean and standard error. (**C**) From the 2,000 frames (60 s recording) of *in vivo* imaging data, a small fluorescent particle was selected and examined how much the image moved during the 60 s. The fluorescent image in the center represents the average of 2,000 frames. The images were projected by averaging in the X- and Y-axis directions. The histograms show the distribution of the centroid in each frame. The standard deviations of the centroid were X: 0.36 and Y: 0.315 µm. (**D**) Example of GECI expression by the fibroin-AAV method. Left: A slice of cerebral cortex applied the fibroin-AAV expression method. Red and blue indicate fluorescence from XCaMP-R and DAPI, respectively; XCaMP-R was expressed not only in layer 2/3 cells but also in layer 5 cells. Center and right. Magnified views of the layers 2/3, and 5 in the left figure (cyan squares), respectively. Please click here to download this File.

Supplementary File 1: (A) Expression efficiency of the wrap with the fibroin-AAV film method and (B) Evaluation of the point spread function during two-photon imaging. Please click here to download this File.

Discussion

This article presents an inexpensive method of creating a large cranial window using a PVDC plastic wrap, transparent silicone, and cover glass. Using this method, we showed that wide-field calcium imaging could be performed over a wide area of the cerebral cortex. Two-photon calcium imaging can be performed from several different cortical regions in the same mouse that has undergone wide-field imaging. Furthermore, it has been shown that a fibroin-AAV film on the plastic wrap used for the window could express GECI over a wide area of the cortex.

Critical steps

It is important to avoid infection and damage to the brain when making cranial windows using plastic wrap. In these conditions, neural and glial activity cannot be observed, and imaging of deeper areas is impossible. Injury to blood vessels also results in bleeding, making imaging impossible due to blood. To avoid infection, making the brain surface and the wrap attached as tightly as possible is critical by sucking out the ACSF. Mannitol administration is important to avoid brain and blood vessel damage by preventing increased brain pressure during surgery. This maintains the space between the surface of the brain and the dura mater and prevents the brain and blood vessels from being touched during the

removal of the skull and dura mater. A stereo microscope with high magnification and tweezers with sharp tips are also effective for accurate surgery.

In the fibroin-AAV method, it is essential to use flesh silkworm cocoons, not to freeze fibroin solution, to dry the fibroin-AAV solution sufficiently, and to apply enough volume of solution (5 µL per 3 mm diameter). When older cocoons were used, expression efficiency was lower. This is because fibroin from old cocoons may be denatured easily. When fibroin solution was frozen at -80 °C and thawed at the time of use, expression efficiency was poor. This may be due to the denaturation of the protein due to freezing and thawing. Since fibroin solutions stored at 4 °C can be effectively used until gelation, it is recommended that fibroin solutions are kept refrigerated and purified from cocoons again after gelation. The fibroin-AAV solution should be dried for at least 3 h, as the expression is poor after less than 3 h. Finally, the area of expression depends on the amount of fibroin-AAV solution used. In the example in **Figure 3M**, the amount was small (5 µL); thus, the fibroin-AAV film only covered the upper half of the window, resulting in non-uniform expression over the window. If a sufficient amount of fibroin-AAV is used, the expression will be uniform over the whole window.

Modifications of the technique

The novel cranial window technique allows one to examine the macroscopic activity of cortical circuits and their underlying single-cell-level activity in the same mouse. Thus, the method can be applied to a variety of neuroscience studies. For example, it can be used to observe cortical activity during decision-making tasks, motor learning, and in mouse models of brain injury and disease. We also believe that the method can be applied not only to rodents but also to non-human primates.

This paper demonstrates that the large cranial window is effective for imaging transgenic mice and mice injected with AAV expressing functional proteins. In particular, it is shown that the fibroin-AAV film on the wrap is much easier than a conventional AAV injection method to express GECIs across the wide area of the cortex. Using a mixture of two AAVs encoding GECIs of different colors[41], the correlation between neuron and glial cell activity can be simultaneously imaged over a wide area of the cortex. Furthermore, the fibroin-AAV film method can also be applied to other genetically-encoded biosensors[42,43,44,45,46,47].

The larger cranial window, which can image both hemispheres, is also possible. Two-photon microscopes with a much wider field of view (~25 mm^2) have recently been developed[25,26,27,28,29]. Combining this two-photon imaging technique with one-photon wide-field imaging using the wide cranial window described here will allow us to examine the relationship between population activity and single-cell activity from unprecedented scales.

Limitations

The food wrap does not allow any substances to pass through. This makes the method difficult to be used for pharmacological experiments. It is also difficult to remove the wrap, making it impossible to insert a glass pipette or electrode. Therefore, it is hard to implement experiments combined with other methods such as simultaneous calcium imaging and electrophysiological recordings, and local administration of drugs using a glass pipette. A possible solution for these limitations is to use the wrap and glass window with a hole. This allows access to the brain *via* a glass pipette or a recording electrode while keeping the cranial window sterile for a long period[48].

Disclosures

The authors have nothing to disclose.

Acknowledgments

This work was supported by Grant-in-Aid for Transformative Research Areas (A) 'Glial Decoding' (JP21H05621 to SM), JSPS KAKENHI (JP19K06883 to SM, 15KK0340 to ES, JP22H00432, JP22H05160, JP17H06312 to HB, and JP17H06313 to KK), Grant-in-Aid for Brain Mapping by Integrated Neurotechnologies for Disease Studies (Brain/MINDS) (JP19dm0207079h0002 to SM, JP19dm0207079 to HB, and JP19dm0207080 to KK), Narishige Neuroscience Research Foundation (to SM), Grant for Young Researcher from Yamanashi Prefecture (to SM), and Takeda Science Foundation (to SM) and partially supported by The Frontier Brain Research Grant from Univ. Yamanashi.

We thank N. Yaguchi and K. Okazaki for animal care and technical assistance and members of the Kitamura lab for helpful discussions.

References

1. Ren, C., Komiyama, T. Wide-field calcium imaging of cortex-wide activity in awake, head-fixed mice. *STAR Protocols.* **2** (4), 100973 (2021).
2. Couto, J. et al. Chronic, cortex-wide imaging of specific cell populations during behavior. *Nature Protocols.* **16** (7), 3241-3263 (2021).
3. Kauvar, I. V. et al. Cortical Observation by Synchronous Multifocal Optical Sampling Reveals Widespread Population Encoding of Actions. *Neuron.* **107** (2), 351-367 e319 (2020).
4. Clancy, K. B., Orsolic, I., Mrsic-Flogel, T. D. Locomotion-dependent remapping of distributed cortical networks. *Nature Neuroscience.* **22** (5), 778-786 (2019).
5. MacDowell, C. J., Buschman, T. J. Low-dimensional spatiotemporal dynamics underlie cortex-wide neural activity. *Current Biology.* **30** (14), 2665-2680 e8 (2020).
6. Makino, H. et al. Transformation of cortex-wide emergent properties during motor learning. *Neuron.* **94** (4), 880-890 e8 (2017).
7. Murphy, T. H. et al. Automated task training and longitudinal monitoring of mouse mesoscale cortical circuits using home cages. *eLife.* **9**, 559654 (2020).
8. Rynes, M. L. et al. Miniaturized head-mounted microscope for whole-cortex mesoscale imaging in freely behaving mice. *Nature Methods.* **18** (4), 417-425 (2021).
9. Cardin, J. A., Crair, M. C., Higley, M. J. Mesoscopic imaging: Shining a wide light on large-scale neural dynamics. *Neuron.* **108** (1), 33-43 (2020).
10. Ren, C., Komiyama, T. Characterizing cortex-wide dynamics with wide-field calcium imaging. *The Journal of Neuroscience.* **41** (19), 4160-4168 (2021).
11. Hamodi, A. S., Martinez Sabino, A., Fitzgerald, N. D., Moschou, D., Crair, M. C. Transverse sinus injections drive robust whole-brain expression of transgenes. *eLife.* **9**, 53639 (2020).
12. Michelson, N. J., Vanni, M. P., Murphy, T. H. Comparison between transgenic and AAV-PHP.eB-mediated expression of GCaMP6s using in vivo wide-field functional imaging of brain activity. *Neurophotonics.* **6** (2), 025014 (2019).
13. Oomoto, I. et al. Protocol for cortical-wide field-of-view two-photon imaging with quick neonatal adeno-

associated virus injection. *STAR Protocols.* **2** (4), 101007 (2021).

14. Fan, J. T. et al. Video-rate imaging of biological dynamics at centimetre scale and micrometre resolution. *Nature Photonics.* **13** (11), 809-816 (2019).
15. Stuart, G. J., Spruston, N. Dendritic integration: 60 years of progress. *Nature Neuroscience.* **18** (12), 1713-1721 (2015).
16. Grienberger, C., Chen, X., Konnerth, A. Dendritic function in vivo. *Trends in Neurosciences.* **38** (1), 45-54 (2015).
17. Takahashi, N. et al. Locally synchronized synaptic inputs. *Science.* **335** (6066), 353-356 (2012).
18. Kitamura, K., Hausser, M. Dendritic calcium signaling triggered by spontaneous and sensory-evoked climbing fiber input to cerebellar Purkinje cells in vivo. *The Journal of Neuroscience.* **31** (30), 10847-10858 (2011).
19. Manita, S. et al. A top-down cortical circuit for accurate sensory perception. *Neuron.* **86** (5), 1304-1316 (2015).
20. Stobart, J. L. et al. Cortical circuit activity evokes rapid astrocyte calcium signals on a similar timescale to neurons. *Neuron.* **98** (4), 726-735 e724 (2018).
21. Srinivasan, R. et al. Ca(2+) signaling in astrocytes from Ip3r2(-/-) mice in brain slices and during startle responses in vivo. *Nature Neuroscience.* **18** (5), 708-717 (2015).
22. Shigetomi, E., Patel, S., Khakh, B. S. Probing the complexities of astrocyte calcium signaling. *Trends in Cell Biology.* **26** (4), 300-312 (2016).
23. Tischbirek, C., Birkner, A., Jia, H., Sakmann, B., Konnerth, A. Deep two-photon brain imaging with a red-shifted fluorometric Ca2+ indicator. *Proceedings of the National Academy of Sciences of the United States of America.* **112** (36), 11377-11382 (2015).
24. Kondo, M., Kobayashi, K., Ohkura, M., Nakai, J., Matsuzaki, M. Two-photon calcium imaging of the medial prefrontal cortex and hippocampus without cortical invasion. *eLife.* **6**, 26839 (2017).
25. Demas, J. et al. High-speed, cortex-wide volumetric recording of neuroactivity at cellular resolution using light beads microscopy. *Nature Methods.* **18** (9), 1103-1111 (2021).
26. Ota, K. et al. Fast, cell-resolution, contiguous-wide two-photon imaging to reveal functional network architectures across multi-modal cortical areas. *Neuron.* **109** (11), 1810-1824 e1819 (2021).
27. Sofroniew, N. J., Flickinger, D., King, J., Svoboda, K. A large field of view two-photon mesoscope with subcellular resolution for in vivo imaging. *eLife.* **5**, 14472 (2016).
28. Stirman, J. N., Smith, I. T., Kudenov, M. W., Smith, S. L. Wide field-of-view, multi-region, two-photon imaging of neuronal activity in the mammalian brain. *Nature Biotechnology.* **34** (8), 857-862 (2016).
29. Yu, C. H., Stirman, J. N., Yu, Y., Hira, R., Smith, S. L. Diesel2p mesoscope with dual independent scan engines for flexible capture of dynamics in distributed neural circuitry. *Nature Communications.* **12** (1), 6639 (2021).
30. Barson, D. et al. Simultaneous mesoscopic and two-photon imaging of neuronal activity in cortical circuits. *Nature Methods.* **17** (1), 107-113 (2020).
31. Wekselblatt, J. B., Flister, E. D., Piscopo, D. M., Niell, C. M. Large-scale imaging of cortical dynamics

during sensory perception and behavior. *Journal of Neurophysiology.* **115** (6), 2852-2866 (2016).

32. Kim, T. H. et al. Long-term optical access to an estimated one million neurons in the live mouse cortex. *Cell Reports.* **17** (12), 3385-3394 (2016).
33. Ghanbari, L. et al. Cortex-wide neural interfacing via transparent polymer skulls. *Nature Communications.* **10** (1), 1500 (2019).
34. Takahashi, T., Zhang, H., Otomo, K., Okamura, Y., Nemoto, T. Protocol for constructing an extensive cranial window utilizing a PEO-CYTOP nanosheet for in vivo wide-field imaging of the mouse brain. *STAR Protocols.* **2** (2), 100542 (2021).
35. Suzuki, T., Murayama, M. Craniotomy for cortical voltage-sensitive dye imaging in mice. *Bio-Protocol.* **6** (3), e1722 (2016).
36. Jackman, S. L. et al. Silk fibroin films facilitate single-step targeted expression of optogenetic proteins. *Cell Reports.* **22** (12), 3351-3361 (2018).
37. Rockwood, D. N. et al. Materials fabrication from Bombyx mori silk fibroin. *Nature Protocols.* **6** (10), 1612-1631 (2011).
38. Jia, H., Rochefort, N. L., Chen, X., Konnerth, A. In vivo two-photon imaging of sensory-evoked dendritic calcium signals in cortical neurons. *Nature Protocols.* **6** (1), 28-35 (2011).
39. Pachitariu, M. et al. Suite2p: beyond 10,000 neurons with standard two-photon microscopy. *bioRxiv.* 061507 (2017).
40. Srinivasan, R. et al. New transgenic mouse lines for selectively targeting astrocytes and studying calcium signals in astrocyte processes in situ and in vivo. *Neuron.* **92** (6), 1181-1195 (2016).
41. Inoue, M. et al. Rational engineering of XCaMPs, a multicolor GECI suite for in vivo imaging of complex brain circuit dynamics. *Cell.* **177** (5), 1346-1360 e1324 (2019).
42. Patriarchi, T. et al. Ultrafast neuronal imaging of dopamine dynamics with designed genetically encoded sensors. *Science.* **360** (6396) (2018).
43. Sun, F. et al. A genetically encoded fluorescent sensor enables rapid and specific detection of dopamine in flies, fish, and mice. *Cell.* **174** (2), 481-496 e419 (2018).
44. Marvin, J. S. et al. An optimized fluorescent probe for visualizing glutamate neurotransmission. *Nature Methods.* **10** (2), 162-170 (2013).
45. Feng, J. et al. A genetically encoded fluorescent sensor for rapid and specific in vivo detection of norepinephrine. *Neuron.* **102** (4), 745-761 e748 (2019).
46. Piatkevich, K. D. et al. Population imaging of neural activity in awake behaving mice. *Nature.* **574** (7778), 413-417 (2019).
47. Sabatini, B. L., Tian, L. Imaging neurotransmitter and neuromodulator dynamics in vivo with genetically encoded indicators. *Neuron.* **108** (1), 17-32 (2020).
48. Roome, C. J., Kuhn, B. Chronic cranial window with access port for repeated cellular manipulations, drug application, and electrophysiology. *Frontiers in Cellular Neuroscience.* **8**, 379 (2014).